Trends and climatic sensitivities of vegetation phenology in semiarid and arid ecosystems in the U.S. Great Basin during 1982-2011

G. Tang[†,†], J. A. Arnone III[†], P. S. J. Verburg[‡], and R. L. Jasoni[†]

[†]Department of Water Resources and Environment, School of Geographical Sciences and Planning, Sun Yat-Sen University, Guangzhou, Guangdong 510275, China

[†]Division of Earth and Ecosystem Sciences, Desert Research Institute, Reno, NV 89512, USA

[‡]Department of Natural Resources and Environmental Science, University of Nevada, Reno, NV 89557, USA

Correspondence to: G. Tang (tangg2010@gmail.com or Universade21@yahoo.com)

Abstract

We quantified the temporal trend and climatic sensitivity of vegetation phenology in dryland ecosystems in the U.S. Great Basin during 1982–2011. Our results indicated that vegetation greenness in the Great Basin increased significantly during the study period, and this positive trend occurred in autumn but not in spring and summer. Spatially, increases in vegetation greenness were more apparent in the northwestern, southeastern, and eastern Great Basin but less apparent in the central and southwestern Great Basin. In addition, the start of growing season (SOS) was not advanced while the end of growing season (EOS) was delayed significantly at a rate of 3.0 days per decade during the study period. The significant delay in EOS and lack of earlier leaf onset caused growing season length (GSL) to increase at a rate of 3.0 days per decade. Interestingly, we found that the interannual variation of mean vegetation greenness calculated for the period of March to November (SSA) was not significantly correlated with mean surface air temperature in SSA but was strongly correlated with total precipitation. On a seasonal basis, the variation of mean vegetation greenness in spring, summer, and autumn was mainly attributable to changes in pre-season precipitation in winter and spring. Nevertheless, climate warming appeared to play a strong role in extending GSL that, in turn, resulted in the upward trend in mean vegetation greenness. Overall, our results suggest that changes in wintertime and springtime precipitation played a stronger role than temperature in affecting the interannual variability of vegetation greenness, while climate warming was mainly responsible for the upward trend in vegetation greenness we observed in Great Basin dryland ecosystems during the 30-year period from 1982 to 2011.

Keywords: Phenology, greenness, leaf senescence, growing season length, climate sensitivity, dryland ecosystems

1 Introduction

Shifts in plant phenology (e.g., greenness, spring leaf onset) resulting from climate change can affect the cycling of carbon, water, and energy between the biosphere and atmosphere (Wu and Liu, 2013), availability of biological and physical resources (White and Nemani, 2011), and best practices for managing these resources for production of fiber and food to sustain human life (Butt et al., 2011). Quantifying the spatiotemporal dynamics of plants phenology – such as long-term trend in vegetation greenness, start of growing season (SOS), end of growing season (EOS), and growing season length (GSL) – and their climatic sensitivity can enable us to assess climate change impacts on terrestrial vegetation dynamics (Soudani et al., 2011) and ecosystem biogeochemistry (Brown et al., 2010). Information about climate-change-associated shifts in vegetation phenology and biogeochemistry in turn has important implications (e.g., defining the period of carbon uptake) for more accurate prediction of terrestrial water, carbon, and nutrient cycles in Earth system, climate, and ecosystem models (e.g., Piao et al., 2011).

Existing phenological studies mostly focus on regions with low evergreen cover such as temperate deciduous forests (e.g., Nagai et al., 2010) or where terrestrial ecosystems may be particularly sensitive to climate warming such as boreal and arctic regions (e.g., Zhang et al., 2011). Only a few studies have focused on quantifying plant phenological responses in semiarid and arid (hereafter dryland) ecosystems to climate variability and recent climate warming (e.g., Bradley and Mustard, 2008; Zhang et al., 2010; Fensholt et al., 2012). Although terrestrial carbon sequestration has been considered to be relatively low in dryland ecosystems, these ecosystems cover almost 40% of Earth's land area (UNDP/UNSO, 1997) and account for nearly 20% of the global soil carbon pool (Field et al., 1998; Lal, 2004). They also may be buffering anthropogenic CO_2 rise more than expected (Jasoni et al., 2005; Wohlfahrt et al., 2008; Poulter et

al. 2014; Ahlström et al., 2015) and are particularly sensitive to both climatic variation (Jasoni et al., 2005; Wohlfahrt et al., 2008) and increasing atmospheric CO_2 concentrations (Jasoni et al., 2005). Hence, quantification of the responses of dryland plant phenology to climate variability at the regional scale is needed to improve forecasting of shifts in ecosystem functioning and consequences for ecosystem services (including livestock grazing, wildlife habitat, and modulation of atmospheric CO_2) that drylands provide.

Climate warming has been widely accepted as the major driver responsible for the general increase in vegetation greenness, earlier SOS, delayed EOS, and the extension of GSL that have occurred in the Northern Hemisphere during the past few decades (e.g., Piao et al., 2011; Hmimina et al., 2013). These findings mainly apply to mesic ecosystems, however, where water is often not limiting for vegetation growth. In dryland ecosystems, water is scarce and the availability of water strongly controls plant seed germination, growth, and reproduction (e.g., Bradley and Mustard, 2005). Although some studies indicated that precipitation plays an important role in affecting vegetation greenness (e.g., Wu and Liu, 2013) and SOS (e.g., Cong et al., 2013) in temperate deserts, it is still unclear if the role of precipitation is as strong as, or even stronger than, that of temperature in controlling plant phenological dynamics in dryland ecosystems. Improved understanding of the role of precipitation in affecting or controlling plant phenology in dryland ecosystems is critical for accurate quantification of terrestrial carbon, water, and plant community dynamics under changing climatic conditions.

The objectives of this study were to utilize the dryland ecosystems at lower elevation zones of the U.S. Great Basin (Fig. 1) to (i) quantify long-term trends in mean vegetation greenness (represented by Normalized Difference Vegetation Index [NDVI]), SOS, EOS, and GSL in the dryland ecosystems that may have occurred during the most recent 30 years of climate warming;

(ii) explore the spatial variation of long-term trends in vegetation greenness; and (iii) examine the climatic sensitivities of trends and variation of vegetation phenology in the study region. To meet these objectives, we utilized satellite-based NDVI data because they enable us to quantify the synoptic and landscape pattern of vegetation phenology (White et al., 2009) as well as its long-term temporal dynamics (Studer et al., 2007). Time series of weather records (temperature and precipitation) were used to analyze climatic sensitivities of vegetation phenology in the study region.

2 Materials and Methods

2.1 Study region

The Great Basin is located in the western United States and encompasses the majority of Nevada (NV), western Utah (UT), and parts of California (CA), Oregon (OR), Idaho (ID), Montana (MT), and Arizona (AZ) (Fig. 1a). It is bordered by the Sierra Nevada Range on the west, the Rocky Mountains on the east, the Columbia Plateau to the north, and the Mojave and Sonoran deserts to the south. The hydrographically defined Great Basin includes the northern Mojave Desert (Grayson, 2011). Lying in the rain shadow of the Sierra Nevada mountain range, the Great Basin is the driest region in the U.S. and experiences extremes of weather and climate that are not normally found elsewhere in the U.S. (Houghton et al., 1975). Most precipitation falls in the winter. Climate conditions inside the Great Basin vary by elevation and latitude, and most of the Basin experiences a semiarid or arid climate with warm summers and cold winters.

Land cover types in the Great Basin are diverse because of topographic and local climatic heterogeneity. The predominant flora in the Great Basin consist of shrubs such as *Artemesia tridentata* (sagebrush), *Ericameria nauseosa* (rabbit brush), *Sarcobatus vermiculatus* (greasewood); grasses such *as Achnatherum hymenoides* (Indian rice grass), *Bouteloua*

curtipendula (Sideoats grama); evergreen trees such as *Pinus monophylla* (pinyon pine) and *Juniperus osteosperma* (Utah juniper); as well as invasive species including *Bromus tectorum* (cheatgrass). In contrast to shrubs and grasses that are mostly present in valleys, evergreens are mainly located in mountain ranges and at higher elevations. Because evergreen forests have little or even no visible leaf seasonal cycle (Botta et al., 2000), they were excluded from this study (see below).

2.2 Satellite-based vegetation indices and data processing

We used the Global Inventory Monitoring and Modeling Studies (GIMMS) NDVI3g data to examine long-term trends in vegetation greenness and phenology. The GIMMS NDVI data were derived from the NOAA Advanced Very High Resolution Radiometer (AVHRR) series satellites (NOAA 7, 9, 11, and 14) and span the period from January 1982 to December 2011 (Tucker et al., 2005). These data are at bi-weekly temporal and 8 km spatial resolution. The data were corrected to remove known non-vegetation effects caused by sensor degradation, clouds, and stratospheric aerosol loading from volcanic eruptions (Tucker et al., 2005). The GIMMS NDVI data have been widely used to quantify long-term trends in vegetation phenology and its relationship to climatic variability at global and continental scales (e.g., Brown et al., 2010; Zhang et al., 2010; Cong et al., 2013). Given that snow cover can affect NDVI values, our analysis excluded winter months (December, January and February) and only considered the period of March to November (spring, summer, and autumn; hereafter, SSA).

To accurately quantify how vegetation phenology in the Great Basin may have changed and responded to climate change during the study period, we refined our study areas based on the Global Land Cover Facility (GLCF) 8 km land cover data (Hansen et al., 2000) and National Land Cover Database (NLCD) 2001 (Homer et al., 2007). We first excluded areas where

evergreen trees predominated in both GLCF and NCLD 2001. In addition, we excluded lakes, urban areas, and cultivated lands defined in either GLCF or NLCD 2001, the phenology of which depends largely on management practices (i.e., irrigation) and crop types. As a result, only areas where shrubs/grasses were predominant in both GLCF and NLCD 2001 (Fig. S1 in Supporting Information) were considered. Finally, we excluded areas located at relatively high elevations (>2100 m), and only selected those at lower elevations (<2100 m; areas where more than 85% of shrubs and grasses are located according to GLCF data) for our analysis (Fig. S1). Fig. 1b shows the distribution of NDVI points considered in this study.

2.3 Weather data and processing

We generally followed the same procedure of acquiring and processing weather data as described in Tang and Arnone (2013). Briefly, we collected time series of daily minimum and maximum temperatures as well as total precipitation from 126 weather stations that are or were historically located within the Great Basin. These stations included the Cooperative Observer Program Stations (COOP), the Remote Automated Weather Stations (RAWS), the SNOwpack TELemetry (SNOTEL) weather stations, and Nevada Test Site (NTS) stations (Fig. 1a). The selection of 126 stations was based on two criteria: first, selected stations had to have at least 24 years of records (80% of coverage during our study period) for each of 12 months during the period of interest in this study; second, selected stations had to be located near selected NDVI points (Fig. 1b). Stations located inside developed areas (e.g., residential), and cultivated land or near urban areas/cities were excluded to maximize the accuracy of climatic sensitivity analysis of vegetation phenology.

For each of the selected stations during the period of interest, daily weather records that exceeded the long-term (1982–2011) mean of all available records from that station by four

standard deviations (for temperature) or greater than 500 mm (for precipitation) were manually checked or removed on a case-by-case basis (Tang and Arnone, 2013). We plotted and visually compared derived time series of monthly minimum and maximum temperatures at each station with those from neighboring stations to further check data inhomogeneity (e.g., Peterson et al., 1998). Daily mean temperature for each station and each day was calculated as the mean of recorded daily minimum and maximum temperatures. Based on these daily values, we calculated mean temperatures for each month, season, and SSA. We used daily total precipitation values from each station to calculate precipitation sums for each month, season, and SSA at each of the selected stations.

2.4 Characterization of temporal dynamics and climatic sensitivities of plant phenology

To quantify long-term trends in vegetation greenness, SOS, EOS, and GSL, we first interpolated the bi-weekly series GIMMS NDVI3g data for all points considered in this study into daily values using a cubic spline interpolation approach. Based on interpolated daily NDVI values, we followed the midpoint-pixel method (White et al., 2009) to define SOS, EOS, and GSL for each NDVI point (Fig. 1b). Instead of using a global threshold, the midpoint-pixel approach uses a locally tuned NDVI threshold to define SOS. This metric has been demonstrated (e.g., White et al., 2009) and also initially tested (see below for detail) to be suitable for semiarid and arid regions. In the midpoint-pixel approach, the state of the ecosystem is indexed by transforming the NDVI to a 0 to 1 $\mathrm{NDVI}_{\mathrm{ratio}}$ as:

$$\mathrm{NDVI}_{\mathrm{ratio}} = \frac{\mathrm{NDVI}-\mathrm{NDVI}_{\mathrm{min}}}{\mathrm{NDVI}_{\mathrm{max}}-\mathrm{NDVI}_{\mathrm{min}}} \quad (1)$$

where NDVI is the interpolated daily NDVI value in a year, and $\mathrm{NDVI}_{\mathrm{max}}$ and $\mathrm{NDVI}_{\mathrm{min}}$ are the maximum and minimum of the NDVI curve. Thus, SOS can be defined as the day of year when a $\mathrm{NDVI}_{\mathrm{ratio}}$ of 0.5 is exceeded because the 0.5 value is often considered to correspond to timing of

the most rapid increase in NDVI or to the initial leafing of the overstory canopy (White et al., 2009). In our study, we defined SOS as the date in a year when the daily $NDVI_{ratio}$ becomes greater than 0.5 for six consecutive days in ascending order, and EOS as the date in a year when the daily $NDVI_{ratio}$ becomes less than 0.5 for six consecutive days in descending order. Annual GSL was calculated as the difference between EOS and SOS. Our initial comparison of SOS based on the midpoint-pixel method with that based on observed breaking leaf buds data (USA National Phenology Network [USA-NPN], 2010) for the study region justified the suitability of this metric in the study region (Fig. S2).

The nonparametric Kendall's tau (τ) based slope estimator (Sen, 1968) was used to compute long-term (1982–2011) or short-term (i.e., a shorter period during 1982–2011) trends in four phenological indices: vegetation greenness, SOS, EOS, and GSL based on their Basin-wide averaged anomalies. We also used this metric to calculate the trends of vegetation greenness at each of the NDVI points to examine the spatial variation of trends of vegetation greenness during 1982–2011. The Kendall's tau method does not assume a distribution for residuals and thus is insensitive to the effect of outliers in time-series data. The two-tailed P-values at the 95% (significant) or 90% (marginally significant) confidence levels were used to test the significance of trends.

This study followed the same procedure described in Tang and Arnone (2013) to calculate a single value for each phenological index for the entire Basin. We first divided the basin into 1.34° × 1.34° boxes to make a total of 37 boxes, each of which (except one) contained at least one weather station (Fig. 1a). We calculated anomalies for each index for each month, season, and SSA at each location (e.g., a NDVI point) against its 30-year arithmetic mean. We then averaged all anomalies within a box to obtain the box anomaly for each index for each month, season, and

SSA. Finally, the resultant box anomalies for each index were averaged to obtain Basin-wide average. The goal of using this approach was to minimize effects of clustered points on the Basin-wide averaged values for each month, season, and SSA. The approaches outlined above also were applied to temperature and precipitation indices.

Based on Basin-wide averaged anomalies, we analyzed the sensitivity of vegetation phenology to changes in temperature and precipitation through the univariate linear regression approach largely because temperature and precipitation correlate/interact with each other. The purpose of this analysis was to examine which variable alone (temperature or precipitation) could better explain interannual variability of vegetation phenology during 1982–2011. The Akaike Information Criterion (AIC; Akaike, 1974) was used to determine the goodness fit of a univariate linear regression model. In addition, locally weighted smoothing (Loess; Cleveland, 1981) was used to predict trends in both phonological indices and climate variables. Regressions the predicted trends in phonological indices against trends in climate variables were used to examine the role of climate factor in affecting long-term trends in vegetation phenology.

Multivariate regression models based on temperature, precipitation, and their interaction were developed to analyze the contribution of variation in temperature, precipitation and their interaction to variations in vegetation phenology during 1982–2011. We used the metric proposed by Lindeman, Merenda, and Gold (LMG; Grömping, 2006) to quantify the relative importance of each regressors (e.g., temperature, precipitation and their product) in controlling the variation of vegetation phenology in the study region. The LMG metric considers both the direct effects of an independent variable (e.g., temperature) on a dependent variable (e.g., greenness) and its indirect effects adjusted by other independent variables (e.g., precipitation) in

a multivariate regression model and thus is suitable for comparing the contribution of variation in temperature and precipitation as well as their interaction to variations in vegetation phenology.

3 Results

3.1 Long-term trends in vegetation greenness and corresponding climatic conditions

When averaged for the period of March to November (i.e., SSA), both mean NDVI and mean surface air temperature in SSA in the dryland ecosystems increased significantly during the period 1982–2011 (Fig. 2a, b) while total precipitation in SSA showed no significant trend during the study period (Fig. 2c). The rate of increase was about 5×10^{-4} ($p<0.04$) units per year in NDVI and 0.2 °C ($p<0.09$) per decade in temperature during 1982–2011. Although mean NDVI in SSA increased during the 1982–2011 period, this long-term positive trend contained shorter periods of increases or decreases in NDVI (Fig. 2a). For example, mean NDVI in SSA decreased significantly ($p<0.01$) from 1986 to 1992 and then increased significantly ($p<0.01$) from 1992 to 1998 (Fig. 2a). Similarly, even though mean surface air temperature showed a long-term positive trend and total precipitation showed no trend in SSA, both temperature and precipitation displayed shorter periods of significant increases or decreases (Fig. 2b, c).

On a seasonal basis, mean NDVI in autumn (Fig. 3c) increased significantly ($p<0.01$) while NDVI in spring and summer (Fig. 3a, b) showed no significant ($p>0.13$) trend during the 1982–2011 period. Mean surface air temperature in spring and autumn (Fig. 3d, f) showed no significant ($p>0.19$) trend while mean temperature in summer (Fig. 3e) increased significantly ($p<0.02$) during the 30-year period. In contrast, total precipitation in spring, summer and autumn showed no significant trends ($p>0.13$) from 1982 to 2011 (Fig. 3g, h, i).

During the 30-year observation period, NDVI, temperature, and precipitation showed a number of shorter-term trends that differed by season. For example, mean springtime NDVI

decreased from 1986 to 1992 (Fig. 3a), whereas mean autumn NDVI increased from 1992 to 1998 (Fig. 3c). In addition, although summertime NDVI showed no significant trend during the period 1982–2011, it decreased significantly ($p<0.01$) from 1982 to 1994 and from 1995 to 2008 (Fig. 3b).

3.2 Spatial heterogeneity of long-term trends in vegetation greenness

Our results indicated that mean SSA NDVI in 39% of the total points (4154) considered in this study had significant ($p<0.05$) predominantly positive trends during 1982–2011. These points with significant trends were located in the northwestern, southern, and eastern Great Basin (Fig. 4a). The rates of increase in mean NDVI in SSA also increased as latitude and longitude increased (Fig. S3). In the central Great Basin, points showing significant long-term trends in NDVI were sparse (Fig. 4a). In addition, both positive and negative trends in mean NDVI in SSA were observed. The number of points where NDVI had a positive trend, however, was triple (30%) those showing a negative trend (10%). The points with a positive trend were concentrated in the southwestern part of the study region or areas near the southern part of the Sierra Nevada Mountains and Death Valley. Overall, points showing significant trends in NDVI in the Great Basin were dominated by the positive trend during the 1982–2011 period (Fig. 4a), especially in the northwestern, eastern, and southeastern Great Basin.

When summarized by each season, the areas where springtime mean NDVI exhibited a positive trend from 1982 to 2011 only accounted for 11%, most of which occurred in the northwestern and eastern Great Basin (Fig. 4b). In the southeastern Great Basin, however, there was still a large portion of areas where NDVI in spring showed a significant positive trend (Fig. 4b). In addition, in spring 12% of all points exhibited a significant negative trend from 1982 to 2011 and most of these points were distributed along a corridor extending from southwest to

northeast of the Great Basin or from areas near the eastern side of the Sierra Nevada mountains to the central and northern Great Basin (Fig. 4b). Summertime mean NDVI showed a significant positive trend in only 9% of the total points considered in this study, and these points were scattered across the Great Basin (Fig. 4c). In 15% of areas considered in this study, summertime mean NDVI decreased during 1982–2011 (Fig. 4c), and most of these points were concentrated in the southern and southwestern Great Basin (Fig. 4c) and near the eastern side of the Sierra Nevada mountains. Autumn mean NDVI increased in 31% of areas during the years 1982–2011, and these increases mostly occurred in the northwestern, eastern, and southeastern Great Basin (Fig. 4d). As in other seasons, there still were points where autumn vegetation greenness decreased significantly during the 1982–2011 period, but these points were less than 9% of the total points considered in our study (Fig. 4d) and mostly concentrated near the eastern side of the Sierra Nevada Mountains.

3.3 Variation of SOS, EOS, and GSL in the Great Basin

Based on the GIMMS NDVI data, the values of the start of growing season (SOS) viewed across the dryland ecosystems of the Great Basin showed no significant ($p=0.59$) trend during 1982–2011 (Fig. 5a), indicating that spring leaf onset was not significantly changed during the study period. In contrast, the end of growing season (EOS) values increased significantly at a rate of 3.0 ($p<0.002$) days per decade during 1982–2011 (Fig. 5b), suggesting that the timing of leaf senescence in the dryland ecosystems was delayed significantly during these years. The non-significant trend toward earlier leaf onset and a significant delay in leaf senescence extended the growing season length (GSL) at a rate of 3.0 ($p<0.05$) days per decade in the dryland ecosystems during 1982–2011 (Fig. 5c).

In addition to these 30-year long-term trends, we observed significant interannual variations in these phenological indicators. For example, the SOS varied on average from Julian day 90 to 111; EOS varied from Julian day 271 to 295; and GSL varied from Julian day 164 to 196 days. Also, the timing of leaf-out and leaf senescence, as well as GSL, did not change monotonically during the 30-year observation period. We also observed shorter-term (decadal or sub-decadal) trends within the 30-year observation period. For example, SOS decreased significantly during the 1982–1990 period but increased significantly during the 1994–2011 period (Fig. 5a).

3.4 Climatic sensitivities of vegetation greenness in the Great Basin

There was no significant relationship ($p=0.53$) between mean SSA NDVI and mean SSA temperature for the non-evergreen lower elevation ecosystems dominated by shrubs and grasses (Fig. 6a). In contrast, mean SSA NDVI was significantly and positively correlated with SSA total precipitation (Fig. 6b). Vegetation greenness (NDVI) increased by 2.0×10^{-4} ($p<0.02$) NDVI units per year when SSA total precipitation increased by an average of 1% per year (about 2.83 mm $year^{-1}$). The calculated AIC values (the smaller the AIC value, the better a univariate regression model fits; Fig. 6) also indicated that interannual variation in SSA total precipitation better explained the interannual variability of mean SSA NDVI during the 1982–2011 period.

Further analyses based on trends in both mean SSA NDVI and surface air temperature suggested, however, that the increase in mean SSA (Fig. 2b) was mainly responsible for the long-term positive trend in mean SSA NDVI (Fig. 6c), which increased by 0.01 ($p<0.001$) units per year when mean annual SSA temperature increased by 1°C. In contrast, the analyses based on trends of both mean SSA NDVI and SSA total precipitation indicated that precipitation did not play a significant ($p=0.64$) role in causing the long-term upward trend in mean SSA NDVI during the study period (Fig. 6d).

On a seasonal basis, interannual variability in mean summertime NDVI was strongly and negatively related to the variation of summertime mean temperature ($p<0.02$) but was not significantly correlated with the variation of summertime total precipitation (Table 1). In spring and autumn, the variation of seasonal mean NDVI was not significantly ($p>0.15$) related to the variations in either seasonal mean temperatures (Fig. 7a) or seasonal total precipitation (Table 1). Nevertheless, the long-term positive trend of mean NDVI in autumn was significantly correlated with the upward trend of autumn temperature, although the trend in autumn temperature was not significant (Fig. 7b).

Compared to temperatures, mean summertime NDVI was positively related to pre-season springtime precipitation sums (PSP) ($p<0.001$). However, mean spring NDVI was not significantly correlated with wintertime precipitation; and mean autumn NDVI was not significantly correlated with summertime precipitation (Table 1). Mean summertime and autumn NDVI were both strongly correlated with wintertime precipitation (Fig. 8). Overall, the calculated AIC values (Table 1) suggested that precipitation in winter and spring played a more important role than temperature in controlling interannual variability of mean spring, summer, and autumn vegetation greenness (Table 1).

3.5 Climatic sensitivities of vegetation phenology in the Great Basin

Our results indicated that the interannual variability of SOS was significantly ($p<0.001$) related to the variation in mean spring temperatures during the study period (Table 2). The timing of spring leaf-out is likely to occur earlier by 2.7 days per year when springtime mean temperature increases by 1°C (Table 2). In contrast, the interannual variability of EOS was not significantly ($p=0.43$) correlated with the variation in seasonal mean temperature in autumn during the study period (Fig. 7c). As a result, the interannual variation in GSL was positively

correlated with the variation of mean temperature in spring and SSA, although the correlation in spring was only marginally significant ($p<0.10$).

Although annual EOS was not significantly correlated with mean autumn temperature (Fig. 7c), the upward trend in annual EOS corresponded well ($p<0.001$) with the trend of seasonal mean temperature in autumn during 1982–2011 (Fig. 7d). Similarly, although GSL was not significantly correlated with seasonal mean temperature in autumn (Fig. 7e), the upward trend in annual GSL corresponded well ($p<0.001$) with the trend of seasonal mean temperature in autumn 1982–2011 (Fig. 7f). These results suggested that the upward trend in autumn temperature (although non-significant statistically) was responsible for the trends of delayed EOS and extended GSL during 1982–2011 that we observed in the U.S. Great Basin.

4 Discussion

4.1 Long-term trends in vegetation greenness in the Great Basin

The upward trend in mean vegetation greenness in SSA we observed during 1982–2011 in the dryland ecosystems of the Great Basin was consistent with reported trends for similar ecosystems worldwide. Fensholt et al. (2012) suggested that semi-arid areas across the globe experienced an increase in vegetation greenness of about 0.015 NDVI units on average during 1981–2007. Zhang et al. (2010) indicated that growing season NDVI in grasslands in southwestern North America increased from 1982 to 2007. In arid environments of China, monthly average NDVI measured during the growing season also increased during 1982–1999 (Piao et al., 2011). These trans-Northern-Hemispheric findings may have resulted from worldwide warming that has occurred during the last few decades (e.g., Menzel et al., 2011; Zeng et al., 2011; Fensholt et al. 2012). In fact, although the interannual variability of mean SSA NDVI was not significantly correlated with the variation in mean surface air temperature, the

warming trend we observed in autumn (Fig. 3f) was likely the major driver responsible for the significant positive trend we measured in GSL (Fig. 7f), which in turn resulted in the 30-year positive trend in mean NDVI values in SSA (Fig. 9b) that we observed in the dryland ecosystems of the U.S. Great Basin.

Our results, however, contrast with those of Zhang et al. (2010) who reported both a negative trend in NDVI from 1982 to 2007 in shrublands in southwestern North America, as well as an oscillation in NDVI with increases observed from 1982 to 1993 and stronger decreases from 1993 to 2007. These apparent discrepancies may be attributed to differences in both time periods considered and spatial extent of the study regions (the Great Basin vs. southwestern North America) and suggest that dryland ecosystems in more northern regions of the arid western U.S. may respond differently to warming trends than those distributed in more southern regions of the arid U.S. as indicated in our study (e.g., Fig. S3a). Such regional differences are actually common (e.g., Jeong et al., 2011) and may be attributable to latitudinal differences in solar radiation and climate conditions, such as decreasing temperature with increasing latitude (Fig. S4a).

The non-significant relationship between the variations of seasonal mean NDVI and mean temperature in autumn in the dryland ecosystems suggested that other factors also played an important role in regulating interannual variability of vegetation greenness in autumn. Multivariate regression analyses suggested that precipitation in winter and autumn, as well as mean temperature in SSA, were responsible (at the 98% confidence level) for the interannual variability of mean NDVI in autumn (Table 3). Increases in surface air temperature in autumn can extend GSL (Fig. 8a), and this temperature effect may be amplified if increased precipitation enhances soil water content. This combination likely would stimulate vegetation growth later

into autumn than under drier conditions. The significant positive relationships between trends in both autumn temperature and GSL (Fig. 7f) as well as between trends in both autumn temperature and NDVI (Fig. 7b) indicated that warming in autumn (although not significant) was likely a major modulating factor for the long-term upward trend of mean autumn NDVI in the study region.

The absence of an observable trend in mean summertime NDVI may have been caused by the combination of an increase in summertime temperature and no change in precipitation (Fig. 3e, h). This combination of conditions may have led to greater limitations (e.g., increased heat stress and resulting soil moisture limitations) on plant growth in summer. Additionally, the strong negative relationship we saw between mean temperature and NDVI in summer contributed to the non-significant relationship between mean temperature and NDVI in SSA (Fig. 6a). The absence of a trend in mean springtime NDVI may have been resulted from a lack of trend in mean springtime temperature, which did not increase significantly during the study period (Fig. 3d). Overall, the significant and non-significant relationships we quantified between NDVI and precipitation and between NDVI and temperature in SSA (Fig. 6a) suggest that changes in precipitation played a more important role than temperature in controlling interannual variability of mean vegetation greenness at lower elevation zones of the U.S. Great Basin.

4.2 Spatial heterogeneity of trends in vegetation greenness in the Great Basin

The trend of increasing NDVI with time as latitude and longitude increase (longitude is negative; Fig. S3) likely resulted from temperature and precipitation gradients along the latitudinal and longitudinal directions (Fig. S4). In the northern Great Basin, temperature was lower compared to other regions and can limit vegetation growth in spring. Thus, it was not surprising that the warming trends that we found appeared to more strongly benefit vegetation

growth at higher latitudes than it did at lower latitudes in the Great Basin, especially in spring and autumn (Fig. S4a). Zhu et al. (2011) also found that the spatial pattern of vegetation phenology in North America depended strongly on latitude. Further, the spatially uniform increases in NDVI we observed in autumn (Fig. 4d) may have occurred as a result of precipitation generated by large-scale frontal systems that generally start in October and can create relatively uniform water additions to the entire region during the autumn (Weiss et al., 2004). In the absence of these large regional inputs of precipitation, we expected that the temporal trend in NDVI would be spatially more variable across the Great Basin (Bradley and Mustard, 2008; Atkinson et al., 2011) than we actually observed (i.e., most points in Fig. 4a are green showing significantly positive trends).

The phenological cycles of leaf onset and senescence as well as effects of climate on vegetation greenness are vegetation- and location-dependent (Atkinson et al., 2011). In the western U.S., topography strongly modulates temperature and precipitation (Hamlet et al., 2007), and local-scale processes – such as cold air drainage flow or the trapping of cold dense air masses by mountains – cause surface climate conditions to vary through space (Daly et al., 2010; Pepin et al., 2011). Because of the spatial heterogeneity of precipitation timing and magnitude, and because historical trends in temperature at the local scale also varied across the Great Basin (Tang and Arnone, 2013), not all points showed significant positive or negative trends in vegetation greenness during 1982–2011 (Fig. 4). Bradley and Mustard (2008) indicated that trends in vegetation greenness in mountainous areas can significantly differ from those in valleys in the Great Basin because valley ecosystems tend to be more resilient than montane ecosystems to severe drought.

4.3 Variation of SOS, EOS, and GSL in the Great Basin

The lack of a 30-year trend in SOS was consistent with field observations in the Great Basin during 1982–1994, which also showed no significant trend (p=0.40) (Fig. S2). Our estimates of SOS averaged 101 Julian days during 1982–1994, only two days greater than that estimated from field observations (99 Julian days). However, our inability to find a trend in SOS contrasts with results from other field observations, satellite-based data, and synthetic studies conducted at regional or continental scales. For example, satellite observations revealed three to eight days advance in spring phenology in northern latitude mesic ecosystems from 1982 to 1991 (Myneni et al., 1997), and a 6.4 day advance from 1982 to 1999 in Eurasian forests (Zhou et al., 2001). Synthesis studies of long-term, in situ observations have identified a widespread trend toward earlier spring in the Northern Hemisphere (e.g., Parmesan and Yohe, 2003). The underlying reasons for these contrasting observations is that springtime mean temperature in the Great Basin did not increase significantly during the study period (Fig. 3d) while spring warming was more significant at high latitudes of the Northern Hemisphere.

Our finding of 3.0 days delay per decade in leaf senescence (EOS) in the Great Basin during 1982–2011 (Fig. 5b) is consistent with patterns from global studies, showing slight larger-scale Northern Hemispheric delays in EOS (0.3 to 1.6 days per decade; Menzel, 2011) and larger North American delays in EOS (1.3 to 8.1 days per decade; Jeong et al., 2011; Zhu et al., 2011) under warmer conditions. In addition, attribution of the extension of GSL mainly to delayed leaf senescence, rather than to earlier leaf onset, also agrees with findings reported in some previous studies (e.g., Zhu et al., 2011). Nevertheless, the non-significant relationship between annual EOS and autumn temperature (Table 2) suggests that the sensitivity of leaf senescence in dryland ecosystems to temperature may differ from temperate and boreal forests where water availability is often not limited. The lack of sensitivity of EOS in the Great Basin to autumn temperature (Fig.

3c) might involve interactive effects of temperature and soil water availability that signal plants to senesce in a way that differs from temperate and boreal forests as demonstrated by the multivariate regression analysis (Table 3; the three regressors for autumn NDVI are all marginally significant at the 90% confidence level). In fact, synoptic scale rains in autumn in these dryland ecosystems can increase the variability of NDVI (Fig. S5), and thus likely alter the timing of leaf senescence in autumn.

4.4 Climatic sensitivities of vegetation phenology in the Great Basin

Previous studies demonstrated that changes in plant phenology in the mid- and high-latitudes of the Northern Hemisphere were primarily linked to temperature variations through adaptive responses of vegetation (e.g., Hmimina et al., 2013). Thus, earlier leaf onset in these regions was believed to result mainly from spring warming (e.g., Kaduk and Los, 2011; Piao et al., 2011). These findings are in accordance with the significant relationship we observed between SOS and mean springtime temperature (Table 2). The non-significant relationships we observed between EOS and mean autumn temperature agreed with earlier findings from European dryland ecosystems. For example, Menzel et al. (2011) reported weak and non-significant correlations between leaf color change in fall and temperature, with the lack of correlation attributed to the sensitivity of vegetation growth in dryland ecosystems to synoptic rainfall events (Fig. S5).

Nevertheless, the good agreement we observed between trends in autumn temperature and EOS (Fig. 7d), as well as between trends in autumn temperature and GSL (Fig. 7f), suggest that regional warming in autumn may likely be the main cause for delays in EOS and the extension of GSL that we measured in the U.S. Great Basin during 1982–2011 (Table 3). The significant positive relationship we detected between GSL and mean NDVI in SSA indicated that the

extension of GSL resulting from the delay of EOS was mainly responsible for the 30-year upward trend in mean vegetation greenness we observed in the Great Basin (Fig. 9b).

Interannual variability in precipitation also appeared to play a strong, and likely more important, role in controlling interannual variability of vegetation greenness in SSA (the calculated AIC values were smaller for precipitation than for temperature; Fig. 6). On a seasonal basis, calculated AIC values (Table 1) still suggest that precipitation in winter, spring, and summer can better explain the interannual variability in spring, summer, and autumn vegetation greenness. The underlying reason for this is that water availability strongly constrains biotic activity in dryland ecosystems including plant seed germination, growth, reproduction, the emergence of leaf-out, and GSL (e.g., Hadley and Szarek, 1981; Bradley and Mustard, 2005). Because perennial plants in dryland ecosystems often have deep roots, increases in pre-season precipitation that increase soil water content in deep soil layers through soil infiltration, are therefore likely to benefit vegetation growth during the following growing season. Relative importance analyses further indicated that the interannual variability of mean greenness in SSA was largely modulated by precipitation instead of temperature (Table 3), and the interannual variability of seasonal greenness in spring, summer, and autumn was attributable mainly to variation in precipitation (especially winter precipitation) in these seasons, rather than to temperature variability (Table 3).

4.5 Non-climatic factors that may influence vegetation phenology in the Great Basin

Although other factors – such as changes in biological soil crust (Ustin et al., 2009), shifts in land cover at landscape-scales, and invasion of exotic species (e.g., cheatgrass; Bradley and Mustard, 2008) – clearly can affect vegetation phenology in the Great Basin dryland ecosystems studied here, we lack precise information about the spatio-temporal distribution of these factors

in the study region. These determinants of vegetation phenology also require investigation and research funding, especially as they interact with climate variability and climate change affects ecosystem function and the services that these ecosystems provide. Also, although we are confident in our calculation of SOS and EOS, a validation of interpolation of time-series bi-weekly NDVI data to daily values may further enhance the accuracy of SOS and EOS estimates. Finally, because our analysis excluded quantitation of NDVI during winter, and because snowfall and snow cover primarily occur at high elevations, effects of snow cover on NDVI values in our study of low elevation sites were minimal. For example, in the southern and southeastern Great Basin (Fig. 4) where snow rarely occurs in spring and autumn, there were a large number of points showing a significant positive trend in vegetation greenness during 1982–2011. This justifies the robustness of our results given the overall climate warming trend occurred across the Great Basin during the last few decades (Tang and Arnone, 2013).

5 Summary

Based on GIMMS NDVI3g data and from a regional perspective, our results suggested that changes in total precipitation rather than mean surface air temperature in SSA was the major factor controlling interannual variability of mean vegetation greenness in dryland ecosystems of the U.S. Great Basin. On a seasonal basis, pre-season precipitation in winter and spring contributed more to the interannual variability of seasonal mean greenness in spring, summer, and autumn. Nevertheless, climate warming although not significant in autumn was mainly responsible for the extension of GSL – resulting from delayed EOS, which in turn resulted in the 30-year positive trend in mean vegetation greenness in the dryland ecosystems. Overall, our results suggested that both precipitation and temperature played an important but different role in affecting vegetation phenology in the dryland ecosystems of the U.S. Great Basin.

Acknowledgements

This project benefited from the NSF EPSCoR grant for Nevada (NSF Cooperative Agreement EPS-0814372). The NDVI data used in this study were downloadable from http://ecocast.arc.nasa.gov/data/pub/gimms/ and historical weather records were from the U.S. Western Regional Climate Center Data Archive. We greatly appreciate several anonymous reviewers for their constructive comments that have helped improve this manuscript.

References

Ahlström, A., Raupach, M.R., Schurgers, G., Smith, B., Arneth, A., Jung, M., Reichstein, M., Canadell, J.G., Friedlingstein, P., Jain, A.K., Kato, E., Poulter, B., Sitch, S., Stocker, B.D., Viovy, N., Wang, Y.P., Wiltshire, A., Zaehle, S. and Zeng. N.: The dominant role of semi-arid ecosystems in the trend and variability of the land CO_2 sink, Science, **348**, 895-899, 2015.

Akaike, H.: A new look at the statistical model identification, IEEE T. Automat. Contr., **19**, 716–723, 1974.

Atkinson, P. M., Jeganathan, C., Dash, J. and Atzberger, C.: Inter-comparison of four models for smoothing satellite sensor time-series data to estimate vegetation phenology, Remote Sens. Environ., **123**, 400-417, 2011.

Botta, A., Viovy, N., Ciais, P., Friedlingstein, P. and Monfray, P.: A global prognostic scheme of leaf onset using satellite data, Glob. Change Biol., **6**, 709-725, 2000.

Bradley, B. A. and Mustard, J. F.: Comparison of phenology trends by land cover class: a case study in the Great Basin, USA, Glob. Change Biol., **14**, 334-346, 2008.

Bradley, B. A. and Mustard, J. F.: Identifying land cover variability distinct from land cover change: cheatgrass in the Great Basin, Remote Sens. Environ., **94**, 204-213, 2005.

Brown, M. E., de Beurs, K. and Vireling, A.: The response of African land surface phenology to large scale climate oscillations, Remote Sens. Environ., **114**, 2286-2296, 2010.

Butt, B., Turner, M. D., Singh, A. and Brottern, L.: Use of MODIS NDVI to evaluate changing latitudinal gradients of rangeland phenology in Sudano-Sahelian West Africa, Remote Sens. Environ.**, 115**, 3367-3376, 2011.

Cong, N., Wang, T., Nan, H., Ma, Y., Wang, X., Myneni, R. B. and Piao S.: Changes in satellite-derived spring vegetation green-up date and its linkage to climate in China from 1982 to 2010: a multimethod analysis, Glob. Change Biol., **19**, 881-891, 2013.

Daly, C., Conklin, D. R. and Unsworth, M. H.: Local atmospheric decoupling in complex topography alters climate change impacts, Int. J. Climatol., **30**, 1857–1864, 2010.

Fensholt, R., Langanke, T., Rasmussen, K., Reenberg, A., Prince, S.D., Tucker, C., Scholes, R.J., Le, Q. B., Bondeau, A., Eastman, R., Epstein, H., Gaughan, A. E., Hellden, U., Mbow, C., Olsson, L., Paruelo, J., Schweitzer, C., Seaquist, J. and Wessels, K.: Greenness in semi-arid areas across the globe 1981-2007 - an Earth Observing Satellite based analysis of trends and drivers, Remote Sens. Environ., **121**, 144-158, 2012.

Field, C. B., Behrenfeld, M. J., Randerson, J. T. and Falkowski, P.: Primary production of the biosphere: Integrating terrestrial and oceanic components, Science, **281**, 237-240, 1998.

Grayson, D. K.: The Great Basin: A natural prehistory, revised and expanded edition, University of California Press, Berkeley and Los Angeles, California, USA. 2011.

Grömping, U.: Relative importance for linear regression in R: The Package relaimpo, J. Stat. Softw., **17**, 1-27, 2006.

Hadley, N. F. and Szarek, S. R.: Productivity of Desert Ecosystems, Bioscience, **31**, 747-753, 1981.

Hamlet, A. F., Mote, P. W., Clark, M. P. and Lettenmaier, D. P.: Twentieth-century trends in runoff, evapotranspiration, and soil moisture in the western United States, J. Climate, **20**, 1468–1486, 2007.

Hansen, M., DeFries, R., Townshend, J. R. G. and Sohlberg, R.: Global land cover classification at 1km resolution using a decision tree classifier, Int. J. Remote Sens., 21, 1331-1365, 2000.

Hmimina, G., Dufrene, E., Pontailler, J. Y., Delpierre, N., Aubinet, M., Caquet, B., de Grandcourt, A., Burban, B., Flechard, C., Granier, A., Gross, P., Heinesch, B., Longdoz, B., Moureaux, C., Ourcival, J.-M., Rambal, S., Saint Andre, L. and Soudani, K.: Evaluation of the potential of MODIS satellite data to predict vegetation phenology in different biomes: An investigation using ground-based NDVI measurements, Remote Sens. Environ., **132**, 145-158, 2013.

Homer, C., Dewitz, J., Fry, J., Coan, M., Hossain, N., Larson, C., Herold, N., McKerrow, A., VanDriel, J. N. and Wickham, J.: Completion of the 2001 National Land Cover Database for the conterminous United States, Photogramm. Eng. Rem. S., **73**, 337-341, 2007.

Houghton, J. G., Sakamoto, C. M. and Gifford R. O.: Nevada's weather and climate. Special Publication 2: Nevada Bureau of Mines and Geology, Mackay Schools of Mines, University of Nevada, Reno, 1975.

Jasoni, R. L., Smith, S. D. and Arnone III, J. A.: Net ecosystems CO_2 exchange in Mojave Desert shrublands during the eight year of exposures to elevated CO_2, Glob. Change Biol., **11**, 749-756, 2005.

Jeong, S. J., Ho, C. H., Gim, H. J. and Brown M. E.: Phenology shifts at start vs. end of growing season in temperate vegetation over the Northern Hemisphere for the period 1982-2008, Glob. Change Biol., **17**, 2385-2399, 2011.

Kaduk, J. D. and Los S. O.: Predicting the time of green up in temperate and boreal biomes, Climatic Change, **107**, 277-304, 2011.

Lal, R.: Carbon sequestration in dryland ecosystems, Environ. Manag., **33**, 528-544, 2004.

Cleveland, W. S.: LOWESS: A program for smoothing scatterplots by robust locally weighted regression. *The American Statistician* **35**, 54, 1981.

Menzel, A., Sparks, T. H., Estrella, N., Estrella, N., Koch, E., Aasa, A., Ahas, R., Alm-kubler, K., Bissolli, P., Braslavska, O., Briede, A., Chmielewski, F. M., Curnel, Y., Dahl, A., Defila, C., Donnelly, A., Filella, Y., Jatczak, K., Mage, F., Mestre, A., Nordli, Y., Penuelas, J., Pirinen, P., Remisova, V., Scheifinger, H., Striz, M., Susnik, A., Van Vliet, A. J. H., Wielgolaski, F. E., Zach, S. and Zust, A.: European phenological response to climate change matches the warming pattern, Glob. Change Biol., **12**, 1969-1976, 2011.

Myneni, R. B., Nemani, R. R., and Running, S. W.: Estimation of global leaf area index and absorbed par using radiative transfer models, IEEE T. Geosci. Remot., **35**, 1380-1393, 1997.

Nagai, S., Nasahara, K. N., Muraoka, H., Akiyama, T. and Tsuchida, S.: Field experiments to test the use of the normalized-difference vegetation index for phenology detection, Agr. Forest Meteorol., **150**, 152-160, 2010.

Parmesan, C. and Yohe, G.: A globally coherent fingerprint of climate change impacts across natural systems, Nature, **421,** 37-42, 2003.

Pepin, N. C., Daly, C. and Lundquist, J.: The influence of surface versus free-air decoupling on temperature trend patterns in the western United States, J. Geophy. Res., **116**, D10109, doi:10.1029/2010JD014769, 2011.

Piao, S., Fang, J., Zhou, L., Ciais, P. and Zhu, B.: Variations in satellite-derived phenology in China's temperate vegetation, Glob. Change Biol., **12**, 672-685, 2011.

Poulter, B., Frank, D., Ciais, P., Myneni, R.B., Andela, N., Bi, J., Broquet, G., Canadell, J.G., Chevallier, Frederic., Liu, Y.Y., Running, S.W., Sitch, S. and van der Werf, G.R.: Contribution of semi-arid ecosystems to interannual variability of the global carbon cycle , Nature, 509, 600-603, 2014.

Sen, P. K.: Estimates of the regression coefficient based on Kendall's Tau, J. Am. Stat. Assoc., **63**, 1379–1389, 1968.

Soudani, K., Hmimina, G., Delpierre, N., Hmimina, G., Hmimina, G., Delpierre, N., Pontailler, J.-Y., Aubinet, M., Bonal, D., Caquet, B., de Grandcourt, A., Burban, B., Flechard, C., Guyon, D., Granier, A., Gross, P., Heinesh, B., Longdoz, B., Loustau, D., Moureaux, C., Ourcival, J.-M., Rambal, S., Saint André, L. and Dufrêne, E.: Ground-based Network of NDVI measurements for tracking temporal dynamics of canopy structure and vegetation phenology in different biomes, Remote Sens. Environ., **123**, 234-245, 2011.

Studer, S., Stockli, R., Appenzeller, C. and Vidale, P. L.: A comparative study of satellite and ground-based phenology, Int. J. Biometeorol., **51**, 405-414, 2007.

Tang, G. and Arnone III, J. A.: Trends in surface air temperature and temperature extremes in the Great Basin during the 20th century from ground-based observations, J. Geophys. Res.–Atmos., **118**, 3579–3589, 2013.

Tucker, C. J., Pinzon, J. E., Brown, M. E., Slayback, D. A., Pak, E. W., Mahoney, R., Vermote, E. F. and N. E. Saleous.: An Extended AVHRR 8-km NDVI Data Set Compatible with MODIS and SPOT Vegetation NDVI Data, Int. J. Remote Sens., **26**, 4485-4498, 2005.

UNDP/UNSO.: Aridity zones and Dryland populations: An Assessment of population Levels in the world's drylands. UNSO/UNDP, New York, 1997.

Ustin, S. L., Valko, P. G., Kefauver, S. C., Santos, M. J., Zimpfer, J. F. and Smith S.: Remote sensing of biological soil crust under simulated climate change manipulations in the Mojave Desert, Remote Sens. Environ., **113**, 317-328, 2009.

Weiss, J. L., Gutzler, D. S., Coonrod, J. E. A. and Dahm, C. N.: Long-term vegetation monitoring with NDVI in a diverse semi-arid setting, central New Mexico, USA, J. Arid Environ., **58**, 249-272, 2004.

White, M. A. and Nemani R. R.: Real-time monitoring and short-term forecasting of land surface phenology, Remote Sens. Environ., **104**, 43-49, 2011.

White, M. A., de Beurs, K. M., Didan, K., Inouye, D. W., Richardson, A. D., Jensen, O. P., O'Keefe, J., Zhang, G., Nemani, R. R., Van Leeuwen, W. J. D., Brown, J. F., Wit, A. D., Schaepman, M., Lin, X., Dettinger, M., Bailey, A. S., Kimball, J., Schwartz, M. D., Baldocchi, D. D., Lee, J. T. and Lauenroth, W. K.: Intercomparison, interpretation, and assessment of spring phenology in North America estimated from remote sensing for 1982-2006, Glob. Change Biol., **15**, 2335-2359, 2009.

Wohlfahrt, G., Fenstermaker, L. F. and Arnone III, J. A.: Large annual net ecosystem CO_2 uptake of a Mojave Desert Ecosystem, Glob. Change Biol., **14**, 1475-1487, 2008.

Wu, X. and Liu, H.: Consistent shifts in spring vegetation green-up date across temperate biomes in China, 1982-2011, Glob. Change Biol., **19**, 870-880, 2013.

Zeng, H., Jia, G., and Epstein, H.: Recent changes in phenology over the northern high latitudes detected from multi-satellite data, Environ. Res. Lett., **6**, 045508 doi:10.1088/1748-9326/6/4/045508, 2011.

Zhang, X., Friedl, M. A. and Schaaf, C. B.: Global vegetation phenology from Moderate Resolution Imaging Spectroradiometer (MODIS), Evaluation of global patterns and

comparison with in situ measurements, J. Geophys. Re.-Biogeo., **111,** 1-14, G04017, DOI: 10.1029/2006JG000217, 2011.

Zhang, X., Goldberg, M., Tarpley, D., Friedl, M. A., Morisette, J., Kogan, F. and Yu, Y.: Drought-induced vegetation stress in southwestern North America, Environ. Res. Lett., **5**, 1-11, 024008 DOI: 10.1029/2011JG000217, 2010.

Zhou, L.M., Tucker, C. J., Kaufmann, R. K., Slayback, D., Shabanov, N. V. and Myneni, R. B.: Variations in northern vegetation activity inferred from satellite data of vegetation index during 1981 to 1999, J. Geophys. Res., **106**, 20069–20083. DOI: 10.1029/2000JD000115, 2001.

Zhu, W., Tian, H., Xu, X., Pan, Y., Chen, G. and Lin, W.: Extension of the growing season due to delayed autumn over mid and high latitudes in North America during 1982-2011, Global Ecol. Biogeogr., **21**, 260-271, 2011.

Tables

Table 1 Linear regression relationship of vegetation greenness to seasonal mean temperature (SMT), total precipitation (STP), and pre-season precipitation (PSP) as well as AIC values.

Seasons	SMT		STP		PSP		AIC†		
	Slope	p<	Slope	p<	Slope	p<	SMT	STP or PSP	PSP
Spring	0.002	0.30	1.1e-4	0.15	1.1e-4	0.18	-162	-167_s	-163_w
Summer	-0.010	**0.01**	1.2e-4	0.16	3.4e-4	**0.001**	-154	-164_s	-154_w
Autumn	0.003	0.29	-5.6e-5	0.23	8.3e-6	0.86	-188	-189_a	-190_w

AIC† refers to the Akaike Information Criterion. The smaller the magnitude of the AIC value, the better a univariate linear regression model fits. The subscripts "w", "s", "a" represent winter, spring, and autumn, respectively.

Table 2 Linear regression relationships of SOS, EOS, and GSL to temperatures (T).

Indices	Spring T		Autumn T		AMT†	
	Slope	p<	Slope	p<	Slope	p<
SOS	-2.7	0.001	--	--	-5.0	0.01
EOS	--	--	0.7	0.43	0.2	0.87
GSL	1.8	0.10	0.6	0.68	5.2	0.02

-- excluded for relationship analysis; AMT† -- annual mean temperature.

Table 3 The relative importance of annual/seasonal mean temperature (T) and precipitation (P) to the variation of annual/seasonal mean NDVI based on multivariate regression analyses.

Best multivariate regression model†	Statistics		LMG† for Regressors (R)‡			
	R^2	p<	R_1 (%)	R_2 (%)	R_3 (%)	R_4 (%)
$SSA_N = SSA_T + SSA_P + SSA_T \times ANN_P$	0.22	0.09	8	75	17	
$MAM_N = MAM_T + DJF_P + MAM_p$	0.31	0.02	42	19	39	
$JJA_N = JJA_T + DJF_P + MAM_P + JJA_T \times DJF_P$	0.59	0.001	25	29	31	15
$SON_N = DJF_P + SON_P + SSA_T$	0.23	0.07	63	20	17	

† These models were selected based on adjusted--R square and p-values. The subscripts "N", "T", and "P" in each model represent NDVI, temperature, and precipitation, respectively. "SSA", "MAM", "JJA" and "SON" represents the period of March to November, spring, summer and autumn, respectively. LMG† refers to the averaging over orderings of importance proposed by Lindeman, Merenda and Gold (LMG; Grömping, 2006). ‡ The order of regressors corresponds to the order of those variables listed in the multivariate regression model.

Figures

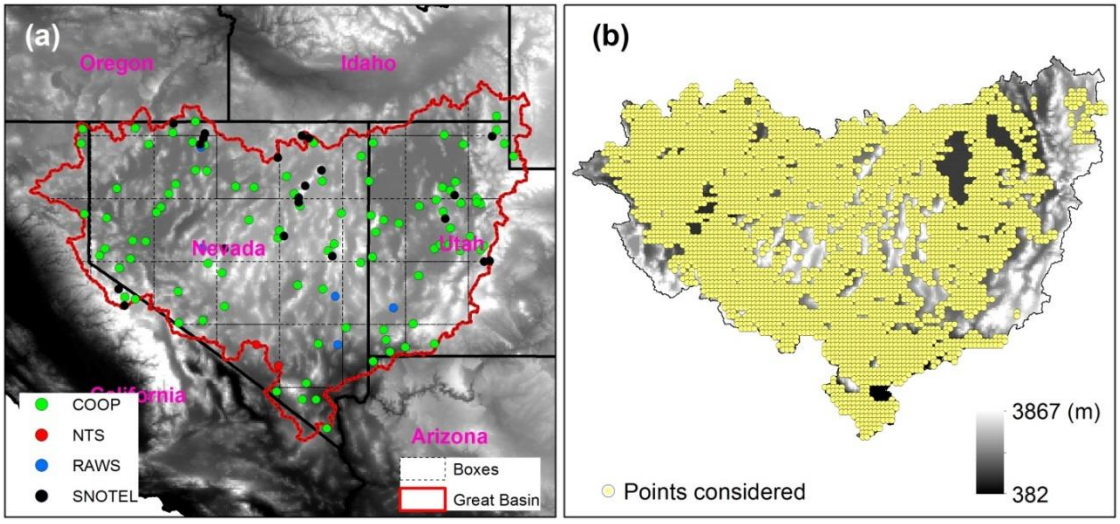

Figure 1. (a) The hydrological Great Basin in the western U.S. and the distribution of weather stations used in this study. (b) The distribution of NDVI points considered in this study.

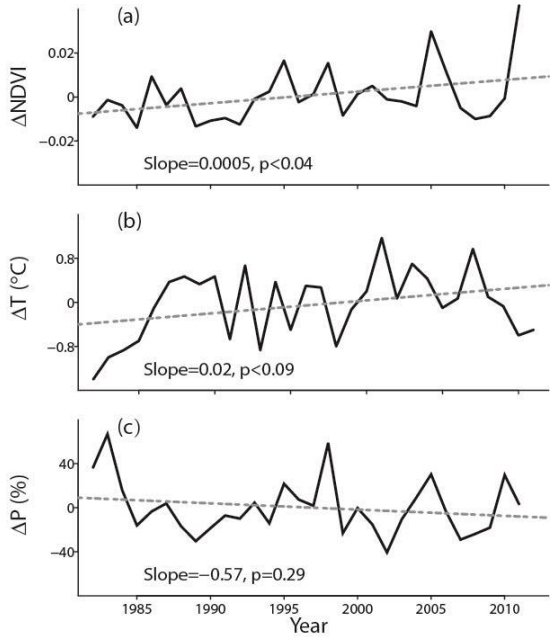

Figure 2. The trends (dashed gray line) and variations (solid black line) of (a) mean NDVI, (b) mean surface air temperature, and (c) total precipitation in the period of March to November in the Great Basin during 1982–2011. Data for y-axis in (a), (b), and (c) are changes relative to their respective long-term (1982–2011) means.

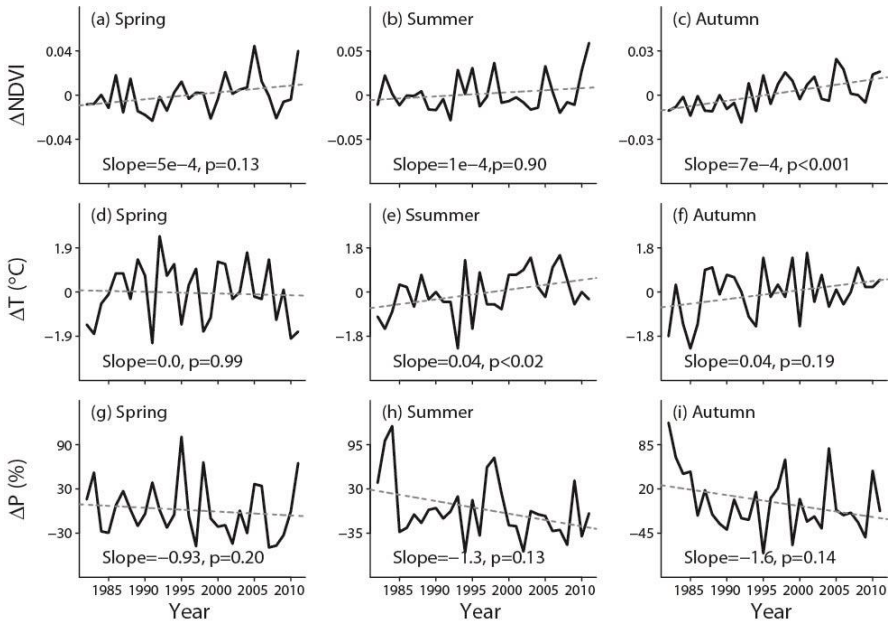

Figure 3. The trends (dashed gray line) and variations (solid black line) of (a) ~ (c) seasonal mean NDVI, (d) ~ (f) seasonal mean temperature, and (g) ~ (i) seasonal total precipitation in the Great Basin during 1982–2011. Data for y-axis are changes relative to their respective long-term (1982–2011) seasonal means.

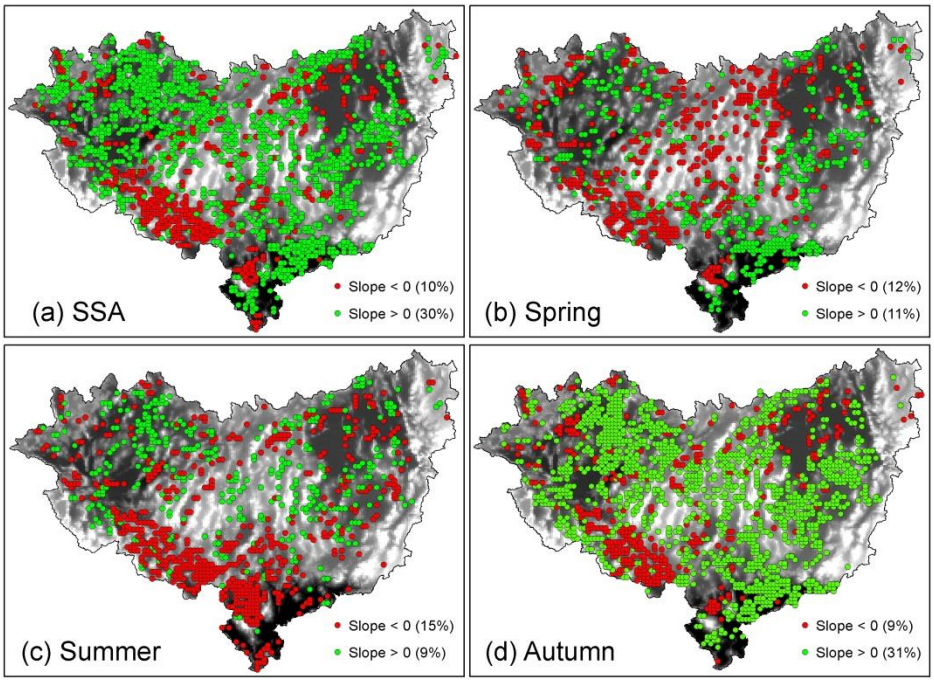

Figure 4. The spatial patterns of statistically significant ($p<0.05$) temporal trends of mean NDVI in (a) SSA (the period of March to November), (b) spring, (c) summer, and (d) autumn during 1982–2011 in the Great Basin. The percentages were calculated against the total of points considered in this study.

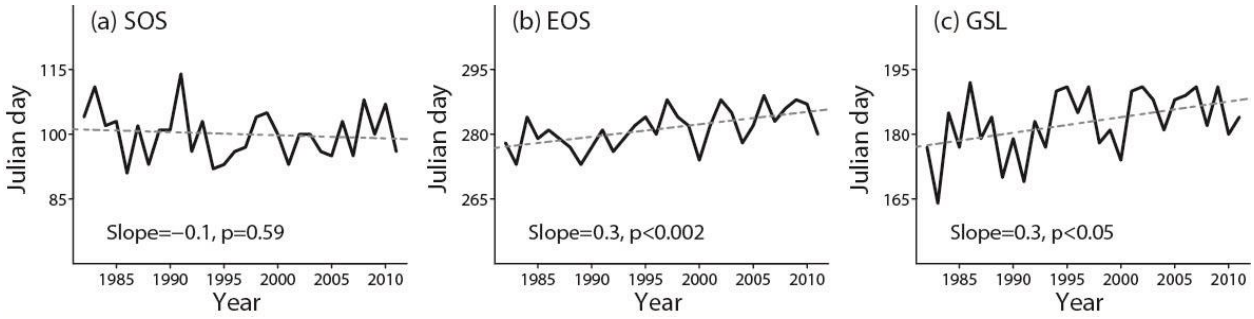

Figure 5. The trends (dashed gray line) and variations (solid black line) in (a) the start of growing season (SOS), (b) the end of growing season (EOS), and (c) the growing season length (GSL) in the Great Basin during 1982–2011.

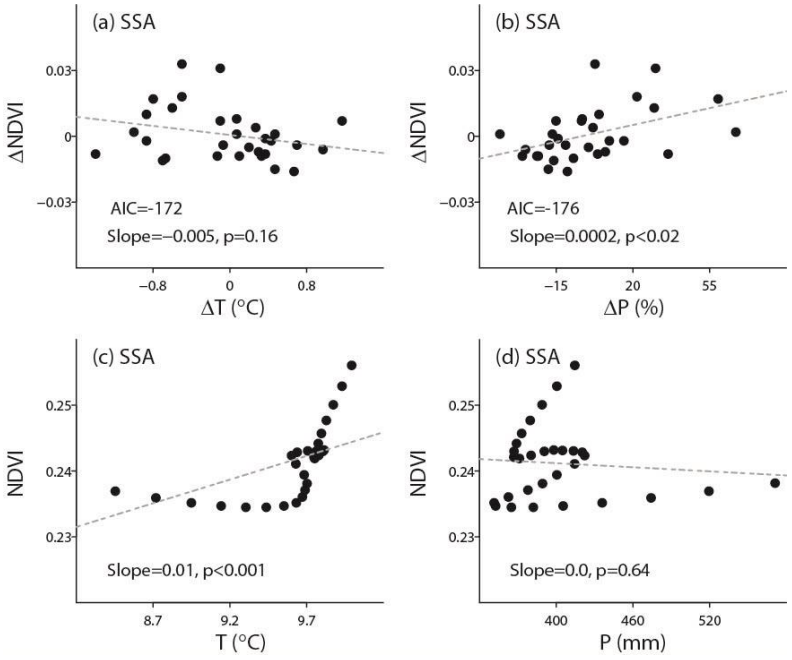

Figure 6. Relationships between (a) mean NDVI and mean surface air temperature in SSA (the period of March to November), (b) mean NDVI and total precipitation in SSA, (c) long-term trends in both mean NDVI and mean surface air temperature in SSA, and (d) long-term trends in both mean NDVI and total precipitation in SSA during 1982–2011. Data shown in (a) and (b) were changes relative to their respective 30-year means. Data shown in (c) and (d) were trends estimated by locally regession smoothing. AIC refers to the Akaike Information Criterion.

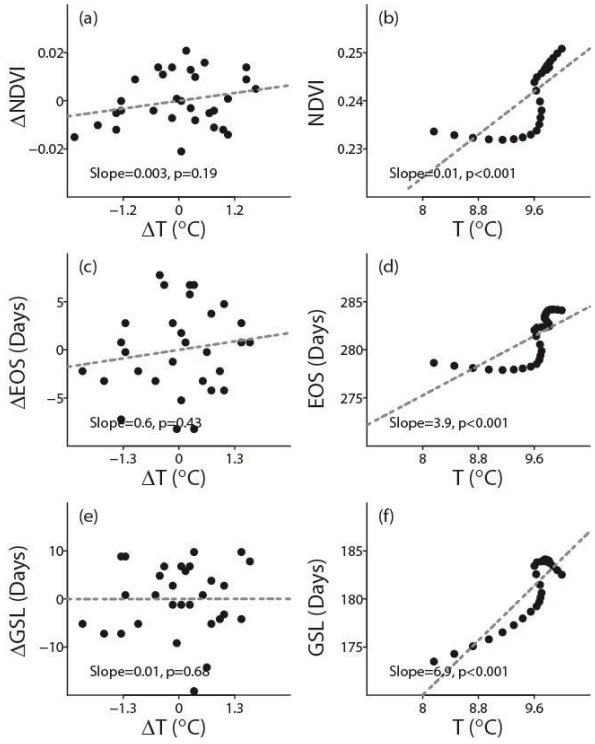

Figure 7. Relationships between (a) mean NDVI and air temperature in autumn, (b) long-term trends in both mean NDVI and air temperature in autumn, (c) EOS and mean air temperature in autumn, (d) long-term trends in both EOS and mean air temperature in autumn, (e) GSL and mean air temperature in autumn, and (f) long-term trends in both GSL and mean air temperature in autumn during 1982–2011. Data shown in (a), (c), and (e) are changes relative to their

respective 30-year means. Data shown in (b), (d), and (f) were trends estimated by locally regession smoothing.

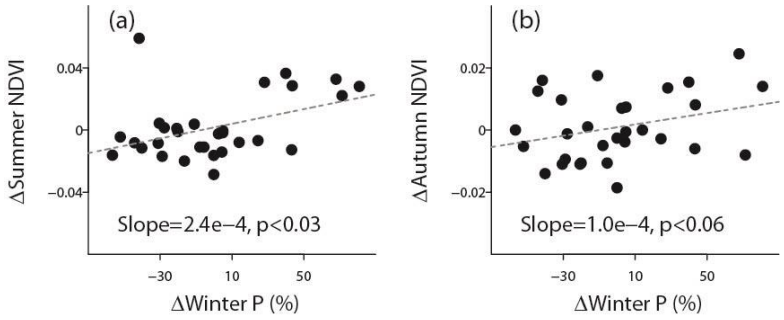

Figure 8. Relationships (a) between mean NDVI in summer and winter precipitation, and (b) between mean NDVI in autumn and winter precipitation during 1982–2011. Data shown in (a) and (b) are changes relative to their respective long-term means.

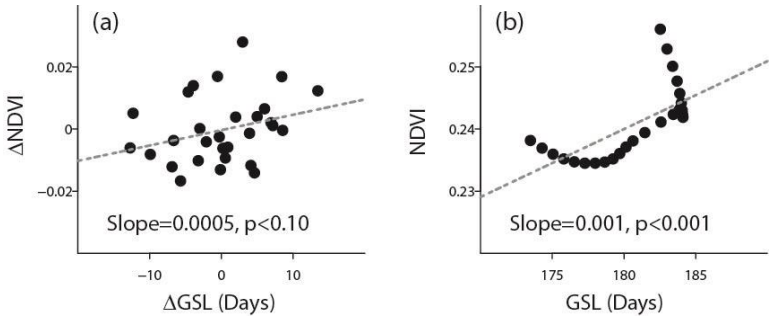

Figure 9. Relationships (a) between mean NDVI in SSA (the period of March to November) and the growing season length (GSL), and (b) between trends in mean NDVI in SSA and GSL during 1982–2011. Data shown in (a) are changes relative their respective long-term means and in (b) are trends estimated by locally regresion smoothing.